Journal of Sound and Vibration 422 (2018) 453–470

Contents lists available at ScienceDirect

Journal of Sound and Vibration

journal homepage: www.elsevier.com/locate/jsvi

Frequency response function-based explicit framework for dynamic identification in human-structure systems

Xiaojun Wei*, Stana Živanović

School of Engineering, University of Warwick, CV4 7 AL, UK

ARTICLE INFO

Article history:
Received 29 April 2017
Received in revised form 22 January 2018
Accepted 9 February 2018

Keywords:
Human-structure interaction
System identification
Human body dynamics
Explicit framework
Frequency response function

ABSTRACT

The aim of this paper is to propose a novel theoretical framework for dynamic identification in a structure occupied by a single human. The framework enables the prediction of the dynamics of the human-structure system from the known properties of the individual system components, the identification of human body dynamics from the known dynamics of the empty structure and the human-structure system and the identification of the properties of the structure from the known dynamics of the human and the human-structure system. The novelty of the proposed framework is the provision of closed-form solutions in terms of frequency response functions obtained by curve fitting measured data. The advantages of the framework over existing methods are that there is neither need for nonlinear optimisation nor need for spatial/modal models of the empty structure and the human-structure system. In addition, the second-order perturbation method is employed to quantify the effect of uncertainties in human body dynamics on the dynamic identification of the empty structure and the human-structure system. The explicit formulation makes the method computationally efficient and straightforward to use. A series of numerical examples and experiments are provided to illustrate the working of the method.

1. Introduction

Dynamic interaction between a human and a low-frequency structure supporting the human is a well-recognised phenomenon that has become increasingly prominent over the last two decades due to the increase in slenderness of modern structures [1–4]. Naturally, the dynamic properties of the human-structure system are influenced by the interplay of dynamics of the two subsystems and they differ from those of the structure itself [1–7]. When considering the vertical flexural vibration modes of a structure, the human occupancy is known to cause a shift in the natural frequency and an increase in the damping ratio [3,8–10]. Knowledge of the dynamic properties of both the occupant(s) and the structure is crucial for developing better understanding of the extent of the human-structure interaction and its influence on the dynamic response analysis and vibration control design for structures accommodating humans.

In structural engineering applications, the dynamics of a human are usually described using a single-degree-of-freedom (SDOF) mass-spring-damper model [3,6,9–14]. The dynamics of a structure are often described utilising a spatial model or a modal model (having, say, n DOFs) that can be established using either finite element method or modal analysis [15]. The

* Corresponding author.
E-mail addresses: x.wei.3@warwick.ac.uk (X. Wei), S.Zivanovic@warwick.ac.uk (S. Živanović).

https://doi.org/10.1016/j.jsv.2018.02.015

human-structure system can then be represented by a $n+1$ DOFs model whose modal properties are determined from an eigenvalue analysis, either numerically or analytically [9,15,16].

Key challenge in studying human-structure systems is the identification of the properties of the human model. Several approaches have been proposed for this purpose. For example, Griffin and his colleagues [17,18] estimated the dynamic properties of a human in a standing or sitting posture by curve fitting measured driving-point apparent masses. On the other hand, Foschi et al. [19] estimated the frequency and damping ratio of a human in a standing posture by minimising differences between the computed and measured displacement responses of the human-floor system exposed to a heel-drop impact. Zheng and Brownjohn [6] measured frequency response functions (FRFs) of both the empty structure and the human-structure system. After identifying a SDOF modal model for a vibration mode of interest from the measured FRFs of the empty structure, they combined this model with assumed properties of the human to derive the eigenvalues of the human-structure system. They used a nonlinear optimisation method to identify the properties of the human that result in the best match between the eigenvalues of the human-structure system and the measured counterparts. This procedure was also employed by Shahabpoor et al. [13] to identify a SDOF model for a walking human. Sachse [2] used a similar procedure for identifying the human's dynamic properties, the only difference being that she compared the measured and calculated FRFs of the human-structure system rather than the eigenvalues. This method was also used by Van Nimmen et al. [14] to identify a SDOF model for a stationary crowd. Jones et al. [20] summarised the dynamic properties of the human in a standing posture reported in the literature. The properties vary significantly between individuals: natural frequency was in the range from 3.3 Hz to 10.4 Hz while damping ratio was between 33% and 69%. Human body dynamics are also found to vary with postures [14,18,21].

Most research is devoted to identifying the dynamics of the human body and predicting the dynamics of human-structure systems. These studies were performed with a sole purpose in mind: to develop dynamic models of humans, either standing or sitting, and then to add them to the dynamic model of an empty structure, usually a grandstand, to predict the dynamic response of the human-structure system in sports or music events [10,20,22]. Little attention has been paid to identifying the dynamics of the empty structure provided the dynamics of the human-structure system are known. This scenario is relevant in manually operated impact hammer modal testing in which a hammer operator is present on the structure during data collection. The identification of dynamic properties of the structure routinely neglects the presence of the hammer operator and it assumes that the dynamics of the empty structure are the same as those of the hammer operator-structure system. This assumption might be erroneous since the interaction between a single human and a structure is important in some cases, such as for ultra-lightweight fibre reinforced polymer (FRP) footbridges. Although some existing methods for identifying human body dynamics [2,6,13,14] can also be used, at least in some cases, for the dynamic identification of the empty structure, they are not necessarily convenient to apply.

To the best knowledge of the authors, there does not exist a single theoretical framework which offers both closed-form solutions and flexibility of being used for any of the three applications as and when needed, i.e. the prediction of the dynamics of the human-structure system when the dynamics of individual systems are known, the identification of human body dynamics when the empty structure and human-structure system dynamics are known and the identification of the empty structure when the human and human-structure dynamics are known. This paper proposes a unifying and simple to implement framework for determining the dynamics of any one of the three systems in terms of the dynamics of the other two. The framework provides closed-form solutions for identifying the dynamics of the system under study and therefore does not require utilisation of nonlinear optimisation techniques inherent to some other studies [2,6,13,14]. The framework utilises curve-fitted FRFs (i.e. receptances, mobilities or accelerances) directly as opposed to using FRFs to derive spatial or modal models of the empty structure and the human-structure system required in some other studies [2,6,13,14]. In addition, the second-order perturbation method is utilised to quantify the effect of uncertainties in human body dynamics on the dynamic identification of the empty structure and the human-structure system. The paper focuses on low-frequency structures (i.e. vibration modes with natural frequencies up to about 8 Hz) on which the human-structure interaction is expected to be strongest. In this frequency region, the human is modelled as a SDOF system since only their first vibration mode is likely to interact with the structure. The proposed method is applicable for problems involving humans in any stationary posture (e.g. standing, sitting and crouching to perform the impact hammer test). Future work will be dedicated to generalise the framework for the crowd-structure interaction.

Following this introductory section, Section 2 introduces the novel method in the context of identifying properties of a human-structure system. Use of the proposed method for identifying human body dynamics is presented in Section 3, whilst its use for estimating dynamics of the empty structure is presented in Section 4. Each section is supported by numerical examples and/or experiments. Conclusions are drawn in Section 5.

2. Identification of the dynamics of a human-structure system

This section presents the theoretical framework followed by a numerical example. The proposed framework was inspired by the studies in the research fields of vibration control [23–25] and nonlinear dynamics [26].

2.1. Theoretical framework

The equation of forced vibration of a linear structure having n DOFs may be cast in second order form as

$$\mathbf{M}_s\ddot{\mathbf{x}}_s + \mathbf{C}_s\dot{\mathbf{x}}_s + \mathbf{K}_s\mathbf{x}_s = \mathbf{f}_s \tag{1}$$

where

$$\mathbf{M}_s = \begin{bmatrix} m^s_{11} & \cdots & m^s_{1(n-1)} & m^s_{1n} \\ \vdots & \ddots & \vdots & \vdots \\ m^s_{(n-1)1} & \cdots & m^s_{(n-1)(n-1)} & m^s_{(n-1)n} \\ m^s_{n1} & \cdots & m^s_{n(n-1)} & m^s_{nn} \end{bmatrix}, \mathbf{C}_s = \begin{bmatrix} c^s_{11} & \cdots & c^s_{1(n-1)} & c^s_{1n} \\ \vdots & \ddots & \vdots & \vdots \\ c^s_{(n-1)1} & \cdots & c^s_{(n-1)(n-1)} & c^s_{(n-1)n} \\ c^s_{n1} & \cdots & c^s_{n(n-1)} & c^s_{nn} \end{bmatrix},$$

$$\mathbf{K}_s = \begin{bmatrix} k^s_{11} & \cdots & k^s_{1(n-1)} & k^s_{1n} \\ \vdots & \ddots & \vdots & \vdots \\ k^s_{(n-1)1} & \cdots & k^s_{(n-1)(n-1)} & k^s_{(n-1)n} \\ k^s_{n1} & \cdots & k^s_{n(n-1)} & k^s_{nn} \end{bmatrix}, \mathbf{x}_s = \begin{bmatrix} x^s_1 \\ \vdots \\ x^s_{n-1} \\ x^s_n \end{bmatrix}, \mathbf{f}_s = \begin{bmatrix} f^s_1 \\ \vdots \\ f^s_{n-1} \\ f^s_n \end{bmatrix}.$$

$\mathbf{M}_s, \mathbf{C}_s$ and $\mathbf{K}_s \in R^{n\times n}$ are the mass, damping and stiffness matrices. $\mathbf{f}_s, \mathbf{x}_s, \dot{\mathbf{x}}_s, \ddot{\mathbf{x}}_s \in R^{n\times 1}$ are the external force, displacement, velocity and acceleration vectors, respectively. R denotes the field of real numbers. Dot denotes the derivative with respect to time.

Eq. (1) may be written in Laplace domain as

$$\mathbf{Z}_s(s)\tilde{\mathbf{x}}_s(s) = \tilde{\mathbf{f}}_s(s) \tag{2}$$

where $\mathbf{Z}_s(s) = (\mathbf{M}_s s^2 + \mathbf{C}_s s + \mathbf{K}_s)$, s is the Laplace variable, whilst $\tilde{\mathbf{x}}_s(s)$ and $\tilde{\mathbf{f}}_s(s)$ are the Laplace transforms of displacement and force vectors.

When a stationary human occupies a structure, the structure and the human form a new joint system whose dynamics are influenced by the dynamics of the two individual components. In line with the previous research, the human is modelled as a SDOF system having mass m_h, damping c_h and stiffness k_h. m_h is assumed to represent the full mass of the human, as implemented in some previous studies [11,19,27–30]. Without loss of generality, it is assumed that the human is located at the $n-$ th degree of freedom of the structure. Therefore, the forced-vibration of the human-structure system can be described by

$$\mathbf{M}_{sh}\ddot{\mathbf{x}}_{sh} + \mathbf{C}_{sh}\dot{\mathbf{x}}_{sh} + \mathbf{K}_{sh}\mathbf{x}_{sh} = \mathbf{f}_{sh} \tag{3}$$

where

$$\mathbf{M}_{sh} = \begin{bmatrix} m^s_{11} & \cdots & m^s_{1(n-1)} & m^s_{1n} & 0 \\ \vdots & \ddots & \vdots & \vdots & \vdots \\ m^s_{(n-1)1} & \cdots & m^s_{(n-1)(n-1)} & m^s_{(n-1)n} & 0 \\ m^s_{n1} & \cdots & m^s_{n(n-1)} & m^s_{nn} & 0 \\ 0 & \cdots & 0 & 0 & m_h \end{bmatrix}, \mathbf{C}_{sh} = \begin{bmatrix} c^s_{11} & \cdots & c^s_{1(n-1)} & c^s_{1n} & 0 \\ \vdots & \ddots & \vdots & \vdots & \vdots \\ c^s_{(n-1)1} & \cdots & c^s_{(n-1)(n-1)} & c^s_{(n-1)n} & 0 \\ c^s_{n1} & \cdots & c^s_{n(n-1)} & c^s_{nn}+c_h & -c_h \\ 0 & \cdots & 0 & -c_h & c_h \end{bmatrix},$$

$$\mathbf{K}_{sh} = \begin{bmatrix} k^s_{11} & \cdots & k^s_{1(n-1)} & k^s_{1n} & 0 \\ \vdots & \ddots & \vdots & \vdots & \vdots \\ k^s_{(n-1)1} & \cdots & k^s_{(n-1)(n-1)} & k^s_{(n-1)n} & 0 \\ k^s_{n1} & \cdots & k^s_{n(n-1)} & k^s_{nn}+k_h & -k_h \\ 0 & \cdots & 0 & -k_h & k_h \end{bmatrix}, \mathbf{x}_{sh} = \begin{bmatrix} x^s_1 \\ \vdots \\ x^s_{n-1} \\ x^s_n \\ x_h \end{bmatrix}, \mathbf{f}_{sh} = \begin{bmatrix} f^s_1 \\ \vdots \\ f^s_{n-1} \\ f^s_n \\ 0 \end{bmatrix},$$

Eq. (3) may be expressed in Laplace domain as

$$\mathbf{Z}_{sh}(s)\tilde{\mathbf{x}}_{sh}(s) = \tilde{\mathbf{f}}_{sh}(s) \tag{4}$$

where

$$\begin{aligned} \mathbf{Z}_{sh}(s) &= (\mathbf{M}_{sh}s^2 + \mathbf{C}_{sh}s + \mathbf{K}_{sh}) \\ &= \begin{bmatrix} \mathbf{Z}_s(s)_{n\times n} & \mathbf{0}_{n\times 1} \\ \mathbf{0}_{1\times n} & m_h s^2 \end{bmatrix} + \begin{bmatrix} \mathbf{0}_{(n-1)\times(n-1)} & \mathbf{0}_{(n-1)\times 1} & \mathbf{0}_{(n-1)\times 1} \\ \mathbf{0}_{1\times(n-1)} & (c_h s + k_h) & -(c_h s + k_h) \\ \mathbf{0}_{1\times(n-1)} & -(c_h s + k_h) & (c_h s + k_h) \end{bmatrix} \\ &= \begin{bmatrix} \mathbf{Z}_s(s)_{n\times n} & \mathbf{0}_{n\times 1} \\ \mathbf{0}_{1\times n} & m_h s^2 \end{bmatrix} + \mathbf{u}(s)\mathbf{u}^{\mathrm{T}}(s) \\ &= \mathbf{Z}_{sm}(s) + \mathbf{u}(s)\mathbf{u}^{\mathrm{T}}(s). \end{aligned}$$

In this expression, $\mathbf{u}(s) = \left[\overbrace{0 \quad \cdots \quad 0}^{n-1} \quad \sqrt{c_h s + k_h} \quad -\sqrt{c_h s + k_h}\right]^{\mathrm{T}}$, $(\bullet)^{\mathrm{T}}$ is the transpose of $(\bullet)$. For the sake of clarity, dimensions of some matrices are stated in the equation.

The receptance matrix of the human-structure system is

$$\mathbf{H}_{sh}(s) = (\mathbf{Z}_{sh}(s))^{-1} = \left(\mathbf{Z}_{sm}(s) + \mathbf{u}(s)\mathbf{u}^{T}(s)\right)^{-1}. \tag{5}$$

Let us denote

$$\mathbf{H}_{sm}(s) = \mathbf{Z}_{sm}^{-1}(s) = \begin{bmatrix} \mathbf{H}_s(s) & 0_{n\times 1} \\ 0_{1\times n} & \dfrac{1}{m_h s^2} \end{bmatrix} \tag{6}$$

where $\mathbf{H}_s(s) = \mathbf{Z}_s^{-1}(s)$ is the receptance matrix of the empty structure.

According to the Sherman-Morrison formula [31], the receptance matrix of the human-structure system can be re-written as

$$\mathbf{H}_{sh}(s) = \mathbf{H}_{sm}(s) - \frac{\mathbf{H}_{sm}(s)\mathbf{u}(s)\mathbf{u}^{\mathrm{T}}(s)\mathbf{H}_{sm}(s)}{1 + \mathbf{u}^{\mathrm{T}}(s)\mathbf{H}_{sm}(s)\mathbf{u}(s)}. \tag{7}$$

Therefore, the receptance matrix of the human-structure system can be obtained using the receptance matrix of the empty structure and the mass, damping and stiffness properties of the human.

The $pn-$ th $(p \le n)$ receptance of the human-structure system may be obtained by pre-multiplying and post-multiplying Eq. (7) by $\mathbf{e}_p^{\mathrm{T}}$ and $\mathbf{e}_n$, respectively,

$$h_{pn}^{sh}(s) = \mathbf{e}_p^{\mathrm{T}}\mathbf{H}_{sm}(s)\mathbf{e}_n - \frac{\mathbf{e}_p^{\mathrm{T}}\mathbf{H}_{sm}(s)\mathbf{u}(s)\mathbf{u}^{\mathrm{T}}(s)\mathbf{H}_{sm}(s)\mathbf{e}_n}{1 + \mathbf{u}^{\mathrm{T}}(s)\mathbf{H}_{sm}(s)\mathbf{u}(s)} \tag{8}$$

where $\mathbf{e}_i^{\mathrm{T}}$ is a vector of dimension $(n+1)\times 1,$ whose $i-$ th entry is unity and the other entries are zero.

Due to

$$\mathbf{e}_p^{\mathrm{T}}\mathbf{H}_{sm}(s)\mathbf{e}_n = h_{pn}^{s}(s) \tag{9}$$

$$\mathbf{e}_p^{\mathrm{T}}\mathbf{H}_{sm}(s)\mathbf{u}(s) = \sqrt{c_h s + k_h}\,h_{pn}^{s}(s) \tag{10}$$

$$\mathbf{u}^{\mathrm{T}}(s)\mathbf{H}_{sm}(s)\mathbf{e}_n = \sqrt{c_h s + k_h}\,h_{nn}^{s}(s) \tag{11}$$

and

$$\mathbf{u}^{\mathrm{T}}(s)\mathbf{H}_{sm}(s)\mathbf{u}(s) = (c_h s + k_h)\left(h_{nn}^{s}(s) + \frac{1}{m_h s^2}\right) \tag{12}$$

where $h_{nn}^{s}(s)$ is the direct receptance at the $n-$ th DOF and $h_{pn}^{s}(s)$ is the cross receptance between the $p-$ th output and the $n-$ th input, both related to the empty structure, Eq. (8) now becomes

$$h_{pn}^{sh}(s) = h_{pn}^{s}(s) - \frac{(c_h s + k_h)h_{pn}^{s}(s)h_{nn}^{s}(s)}{1 + (c_h s + k_h)\left(h_{nn}^{s}(s) + \frac{1}{m_h s^2}\right)} \tag{13}$$

which indicates that the $pn-$ th cross receptance of the human-structure system may be calculated using the $h_{nn}^{s}(s)$ and $h_{pn}^{s}(s)$ of the empty structure and the dynamic properties of the human.

If $p = n$, then

$$h_{nn}^{sh}(s) = h_{nn}^{s}(s) - \frac{(c_h s + k_h)h_{nn}^{s}(s)h_{nn}^{s}(s)}{1 + (c_h s + k_h)\left(h_{nn}^{s}(s) + \frac{1}{m_h s^2}\right)} \tag{14}$$

which indicates that the direct receptance of the human-structure system could be calculated using $h^s_{nn}(s)$ of the empty structure and the dynamic properties of the human.

The denominator of Eq. (13) or (14) generates the characteristic equation

$$1 + (c_h s + k_h)\left(h^s_{nn}(s) + \frac{1}{m_h s^2}\right) = 0 \tag{15}$$

from which the eigenvalues (and therefore natural frequencies and damping ratios) of the human-structure system can be calculated.

2.2. Effect of uncertainties in human properties on predicting the dynamics of the human-structure system

The dynamic properties of the human body may vary due to small postural changes and/or changes in vibration response level. These variations inevitably affect the dynamic prediction of the human-structure system. The second-order perturbation method [32] could be used to estimate the effect of the uncertainties. The perturbation method is based on the Taylor series expansion of the system response around the mean value of the input parameters and it is used to compute the expectations and moments of the output parameters.

Here, the small variations in the stiffness and damping of the human body are considered. No variation in the mass is considered since the mass can be measured accurately. It is assumed that the stiffness and damping of the human body are independent normal random variables. The expectation and standard deviation of the stiffness are E_{k_h} and σ_{k_h}, respectively, while for the damping these are E_{c_h} and σ_{c_h}.

The magnitude and phase of the $pn-$ th receptance of the joint system may be expressed as

$$\left|h^{sh}_{pn}(s)\right| = \sqrt{\left(\mathrm{Re}\left(h^{sh}_{pn}(s)\right)\right)^2 + \left(\mathrm{Im}\left(h^{sh}_{pn}(s)\right)\right)^2} \tag{16}$$

and

$$\angle h^{sh}_{pn}(s) = \arctan\left(\frac{\mathrm{Im}\left(h^{sh}_{pn}(s)\right)}{\mathrm{Re}\left(h^{sh}_{pn}(s)\right)}\right) \tag{17}$$

where $|(\cdot)|$ is the magnitude of $(\cdot)$; $\angle(\cdot)$ is the phase of $(\cdot)$; and $\mathrm{Re}(\cdot)$ and $\mathrm{Im}(\cdot)$ are the real and imaginary parts of $(\cdot)$. Eq. (13) infers that the magnitude and phase are functions of the damping and stiffness of the human body. The expectation and standard deviation of the magnitude can be expressed as Eqs. (18) and (19) using the second-order perturbation method [32].

$$E\left(\left|h^{sh}_{pn}(s)\right|\right) \approx \left|h^{sh}_{pn}(s)\right| \Big| \begin{matrix} c_h = E_{c_h} \\ k_h = E_{k_h} \end{matrix} + \frac{1}{2}\left(\frac{\partial^2\left|h^{sh}_{pn}(s)\right|}{\partial c_h^2}\Big| \begin{matrix} c_h = E_{c_h} \\ k_h = E_{k_h} \end{matrix} \sigma^2_{c_h} + \frac{\partial^2\left|h^{sh}_{pn}(s)\right|}{\partial k_h^2}\Big| \begin{matrix} c_h = E_{c_h} \\ k_h = E_{k_h} \end{matrix} \sigma^2_{k_h}\right) \tag{18}$$

and

$$\sigma\left(\left|h^{sh}_{pn}(s)\right|\right) \approx \sqrt{\left(\frac{\partial\left|h^{sh}_{pn}(s)\right|}{\partial c_h}\Big| \begin{matrix} c_h = E_{c_h} \\ k_h = E_{k_h} \end{matrix}\right)^2 \sigma^2_{c_h} + \left(\frac{\partial\left|h^{sh}_{pn}(s)\right|}{\partial k_h}\Big| \begin{matrix} c_h = E_{c_h} \\ k_h = E_{k_h} \end{matrix}\right)^2 \sigma^2_{k_h}} \tag{19}$$

where $E(\cdot)$ is the expectation of $(\cdot)$; $\sigma(\cdot)$ is the standard deviation of $(\cdot)$; $\frac{\partial\left|h^{sh}_{pn}(s)\right|}{\partial z}$ and $\frac{\partial^2\left|h^{sh}_{pn}(s)\right|}{\partial z^2}$ are the first and second-order partial derivatives of $\left|h^{sh}_{pn}(s)\right|$ with respect to z, $(z = c_h \text{ or } k_h)$, respectively.

Similarly, the expectation and standard deviation of the phase can be expressed as,

$$E\left(\angle h^{sh}_{pn}(s)\right) \approx \angle h^{sh}_{pn}(s)\Big| \begin{matrix} c_h = E_{c_h} \\ k_h = E_{k_h} \end{matrix} + \frac{1}{2}\left(\frac{\partial^2 \angle h^{sh}_{pn}(s)}{\partial c_h^2}\Big| \begin{matrix} c_h = E_{c_h} \\ k_h = E_{k_h} \end{matrix} \sigma^2_{c_h} + \frac{\partial^2 \angle h^{sh}_{pn}(s)}{\partial k_h^2}\Big| \begin{matrix} c_h = E_{c_h} \\ k_h = E_{k_h} \end{matrix} \sigma^2_{k_h}\right) \tag{20}$$

and

$$\sigma\left(\angle h^{sh}_{pn}(s)\right) \approx \sqrt{\left(\frac{\partial \angle h^{sh}_{pn}(s)}{\partial c_h}\Big| \begin{matrix} c_h = E_{c_h} \\ k_h = E_{k_h} \end{matrix}\right)^2 \sigma^2_{c_h} + \left(\frac{\partial \angle h^{sh}_{pn}(s)}{\partial k_h}\Big| \begin{matrix} c_h = E_{c_h} \\ k_h = E_{k_h} \end{matrix}\right)^2 \sigma^2_{k_h}} \tag{21}$$

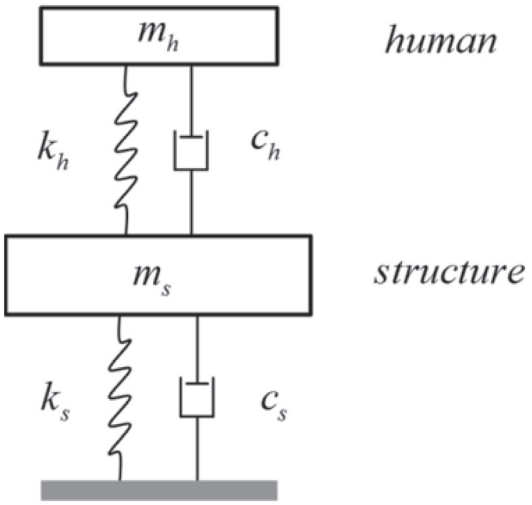

Fig. 1. 2DOF model of human-structure system.

Table 1
Dynamic properties of the human-structure system.

Dynamic property	Empty structure	Human[a]	Human-structure system
Mass (kg)	$m_s = 650$	$m_h = 62$	/
Damping (N·s·m^{-1})	$c_s = 792.31$	$c_h = 1.44 \times 10^3$	/
Stiffness (N·m^{-1})	$k_s = 6.04 \times 10^5$	$k_h = 6.12 \times 10^4$	/
Frequency (Hz)	$f_s = 4.85$	$f_s = 5.0$	$f_1 = 4.51, f_2 = 5.38$
Damping ratio (%)	$\zeta_s = 2.0$	$\zeta_s = 37.0$	$\zeta_1 = 7.3, \zeta_2 = 33.4$
Eigenvalues (s^{-1})	/	/	$\mu_{1,3} = -2.0595 \pm 28.2310$i $\mu_{2,4} = -11.2826 \pm 31.8841$i
Eigenvectors	/	/	$\mathbf{v}_{1,3} = [0.3747 \pm 0.3132\text{i} \quad 1]$ $\mathbf{v}_{2,4} = [-0.0960 \pm 0.1282\text{i} \quad 1]$

[a] The human dynamic properties correspond to the fundamental mode of the human model for standing posture specified in ISO 5982 [33].

2.3. Numerical example: 2DOF human-structure system

Let us consider a SDOF structure occupied by a SDOF human shown in Fig. 1. The dynamic properties of the individual human and the structure as well as those of the human-structure system (obtained from eigenvalue analysis of the 2DOF model) are given in Table 1. The first vibration mode of the human-structure system having frequency f_1 and damping ratio ζ_1 is dominated by structural motion. The second mode (frequency f_2 and damping ratio ζ_2) is dominated by human motion.

If the direct receptance of the empty structure were measured accurately, it would have resulted in

$$h_{11}^{s}(s) = \frac{1}{m_s s^2 + c_s s + k_s} = \frac{1}{650s^2 + 792.31s + 6.04 \times 10^5}. \tag{22}$$

Taking into account that the mass, damping and stiffness of the human body are $m_h = 62$ kg, $c_h = 1.44 \times 10^3$ N·s·m^{-1} and $k_h = 6.12 \times 10^4$ N·m^{-1}, respectively, the direct receptance of the human-structure system $h_{11}^{sh}(s)$ can be calculated from Eq. (14)

$$h_{11}^{sh}(s) = \frac{1}{650s^2 + 792.31s + 6.04 \times 10^5} - \frac{\left(1.44 \times 10^3 s + 6.12 \times 10^4\right)\left(\frac{1}{650s^2+792.31s+6.04\times10^5}\right)^2}{1 + \left(1.44 \times 10^3 s + 6.12 \times 10^4\right)\left(\frac{1}{650s^2+792.31s+6.04\times10^5} + \frac{1}{62s^2}\right)} \tag{23}$$

The characteristic equation

$$1 + \left(1.44 \times 10^3 s + 6.12 \times 10^4\right)\left(\frac{1}{650s^2 + 792.31s + 6.04 \times 10^5} + \frac{1}{62s^2}\right) = 0 \tag{24}$$

generates the eigenvalues of the human-structure system $\mu_{1,3} = -2.0595 \pm 28.2310$i s^{-1} and $\mu_{2,4} = -11.2826 \pm 31.8841$i s^{-1}, which are the same as those shown in Table 1.

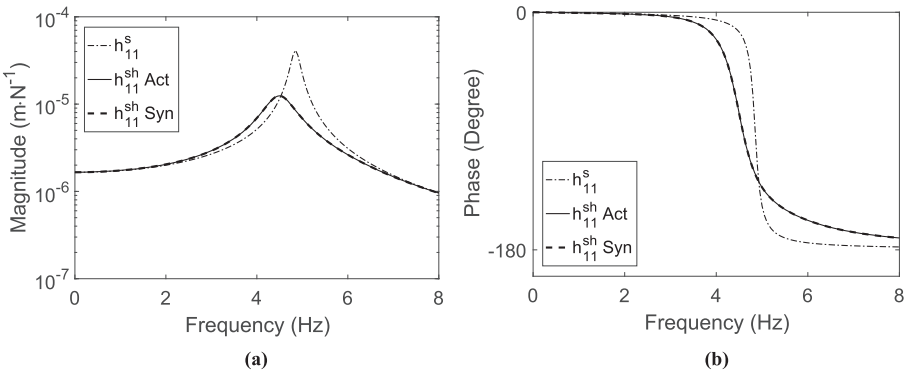

Fig. 2. Receptances of the human-structure system and the structure: (a) Magnitude; (b) Phase.

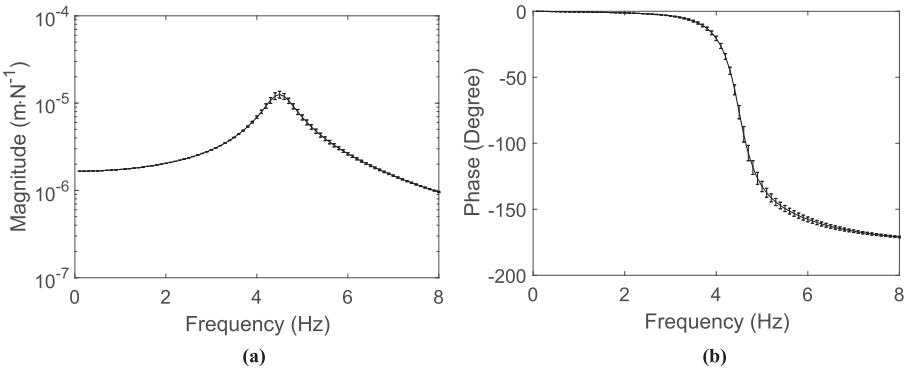

Fig. 3. The direct receptance of the human-structure system: (a) Magnitude; (b) Phase; Solid line - Expectation; Error bar - Standard deviation.

The synthesised direct receptance of the human-structure system described by Eq. (23), shown as the thick dashed line in Fig. 2, accurately reproduces the actual receptance of the human-structure system shown as the thin solid line. Fig. 2 also shows that the presence of the human shifts the frequency from 4.85 Hz for the empty structure (dash-dotted line) to 4.51 Hz for the human-structure system. It also significantly increases the damping ratio of the mode dominated by structural motion (from 2.0% to 7.3%). The mode dominated by human motion is heavily damped which is the reason that it cannot be observed in the receptance graph for the human-structure system. The structure in this example is an actual 16.9 m long glass FRP composite bridge [34]. The example demonstrates that the presence of a single human can significantly modify the dynamics of the empty structure.

Let us assume the expectation and standard deviation of the damping of the human body are $E_{c_h} = 1.44 \times 10^3$ N·s·m^{-1} and $\sigma_{c_h} = 0.1c_h$ N·s·m^{-1}, respectively, while the counterparts for the stiffness are $E_{k_h} = 6.12 \times 10^4$ N·m^{-1} and $\sigma_{k_h} = 0.1k_h$ Nm^{-1} (The corresponding expectations and standard deviations of the frequency and damping ratio are $E_{f_h} = 5.0$ Hz and $\sigma_{f_h} = 0.25$ Hz and $E_{\zeta_h} = 37.0\%$ and $\sigma_{\zeta_h} = 4.0\%$, estimated using the second-order perturbation method [32]). By using the proposed uncertainty estimation method in Section 2.2, the expectation and standard deviation of the direct receptance of the human-structure system can be obtained, as plotted in Fig. 3. The coefficient of variation (CoV) of 10% for both the damping and stiffness of the human body led to the maximum CoV of 9% for the magnitude and phase of the predicted FRF of the human-structure system. The predicted expectations and standard deviations shown in Fig. 3 were verified using Monte Carlo simulations (sample size = 1000).

3. Identification of the dynamics of the human body

In this section, formulas for identifying the dynamics of a stationary human occupying a structure are presented, and their use is demonstrated in an experiment conducted on a laboratory bridge.

3.1. Theoretical derivations

Let us assume that the direct receptance at the $n-$ th DOF h^s_{nn} of the empty structure is available (for example, through modal testing). In addition, let us assume that the direct receptance at the $n-$ th DOF or the cross receptance between the $p-$

th output and the $n-$ th input of the human-structure system is also available resulting in identifying the complex conjugate eigenvalues μ_k^{sh} and $\overline{\mu}_k^{sh}$ of the $k-$ th mode dominated by structural motion of the human-structure system. The eigenvalues μ_k^{sh} and $\overline{\mu}_k^{sh}$ should satisfy Eq. (15), i.e.

$$\begin{bmatrix} c_h \\ k_h \end{bmatrix} = \begin{bmatrix} \mu_k^{sh} & 1 \\ \overline{\mu}_k^{sh} & 1 \end{bmatrix}^{-1} \begin{bmatrix} -\dfrac{\left(\mu_k^{sh}\right)^2 m_h}{\left(\mu_k^{sh}\right)^2 m_h h_{nn}^s\left(\mu_k^{sh}\right)+1} \\ -\dfrac{\left(\overline{\mu}_k^{sh}\right)^2 m_h}{\left(\overline{\mu}_k^{sh}\right)^2 m_h h_{nn}^s\left(\overline{\mu}_k^{sh}\right)+1} \end{bmatrix} \tag{25}$$

Eq. (25) demonstrates that the damping c_h and stiffness k_h of the human can be calculated using the mass of the human m_h and the direct receptance of the empty structure $h_{nn}^s(s)$ that is evaluated at a pair of eigenvalues μ_k^{sh} and $\overline{\mu}_k^{sh}$. Eq. (25) always results in real solutions for c_h and k_h due to the use of the complex conjugate pair μ_k^{sh} and $\overline{\mu}_k^{sh}$.

Making use of the proposed approach for experimental identification of human properties is straightforward. It only requires measuring a direct receptance for the empty structure and a direct receptance or a cross receptance for the human-structure system.

If the measured quantity is accelerance rather than receptance, an alternative form of Eq. (25) should be used. The acceleration $\mathbf{a}(s)$ and the displacement $\mathbf{x}(s)$ are related via $\mathbf{a}(s) = s^2\mathbf{x}(s)$. The receptance matrix $\mathbf{H}^s(s)$ and the accelerance matrix $\mathbf{H}_a^s(s)$ satisfy the relationship

$$\mathbf{H}^s(s) = \frac{\mathbf{H}_a^s(s)}{s^2} \tag{26}$$

leading to the estimate of the damping and stiffness of the human from Eq. (27)

$$\begin{bmatrix} c_h \\ k_h \end{bmatrix} = \begin{bmatrix} \mu_k^{sh} & 1 \\ \overline{\mu}_k^{sh} & 1 \end{bmatrix}^{-1} \begin{bmatrix} -\dfrac{\left(\mu_k^{sh}\right)^2 m_h}{m_h h_{a,nn}^s\left(\mu_k^{sh}\right)+1} \\ -\dfrac{\left(\overline{\mu}_k^{sh}\right)^2 m_h}{m_h h_{a,nn}^s\left(\overline{\mu}_k^{sh}\right)+1} \end{bmatrix} \tag{27}$$

As can be seen from Eqs. (25) and (27), the identification of human body dynamics relies on the quality of the curve fitting of the FRFs of the empty structure and also of the FRFs around the modes dominated by structural motion of the joint system. The strategies for performing curve fitting have been investigated elsewhere, e.g. Refs. [35,36], and have not been elaborated in this paper.

Fig. 4. The empty structure.

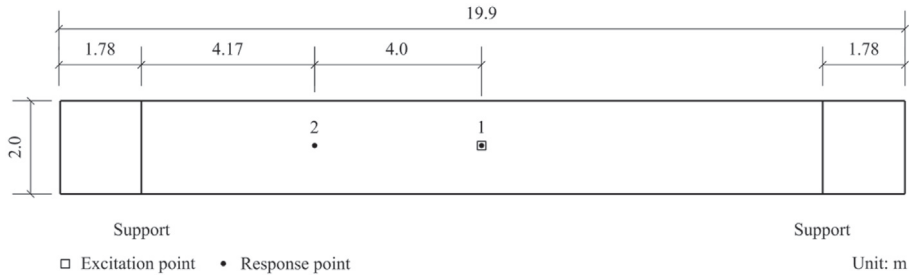

Fig. 5. Bridge geometry and measurement points.

3.2. Experimental case study: dynamic properties of a human in a standing posture

The use of the proposed method is demonstrated on an example of identifying the dynamic properties of a human standing on a steel-concrete composite bridge situated in the Structures Laboratory at the University of Warwick (Fig. 4). The bridge has a mass of 16,500 kg whilst its deck is 19.9 m long and 2 m wide. It sits on two meccano frames that span 16.34 m. The mass of the human is 100 kg and his height is 180 cm. The experiments were approved by the Biomedical and Scientific Research Ethics Committee at the University of Warwick.

Accelerances of the empty bridge and the human-bridge system were measured in a modal testing programme. The measurement points are shown in Fig. 5. The bridge was excited using an electrodynamic shaker (Model APS 400) placed at test point (TP) 1, as shown in Fig. 6. The generated force was indirectly measured using an accelerometer (Honeywell QA750) of nominal sensitivity 1300 mV/g attached to the moving armature. Another two accelerometers of the same type were placed at TP1 and TP2 to measure the vibration responses of the bridge in the vertical direction. The data acquisition system consisted of a laptop, a 4-channel data logger (SignalCalc Ace by Data Physics), a signal conditioner and a power amplifier (Model APS 145). A chirp signal in the frequency range 1–9 Hz was applied to the structure for 64 s. A data acquisition window was set to 128 s. No window was used in data processing since the vibration responses returned to the ambient level within the data acquisition window. Six averages were used to minimise the effects of noise. The typical standing posture of the human is shown in Fig. 6.

3.2.1. Modal testing

The dynamic properties of the human body were identified at three different force levels. The induced maximum accelerations at the driving point on the empty bridge and the human-bridge system ranged from 0.36 $m \cdot s^{-2}$ to 0.65 $m \cdot s^{-2}$ and from 0.34 $m \cdot s^{-2}$ to 0.62 $m \cdot s^{-2}$, respectively. The frequencies and damping ratios of the empty structure showed negligible variation with the response level. The same conclusion was drawn for the human-structure system. These findings suggest that the empty bridge and the human-bridge system exhibited relatively linear behaviour at the three different force levels and they all resulted in almost the same properties of the human body. The force level chosen for presentation in this paper is shown in Fig. 7 whilst the corresponding vibration response at TP1 for the unoccupied bridge is shown in Fig. 8. The direct and cross accelerances for the empty bridge and the bridge occupied by the test subject are shown in Figs. 9 and 10, respectively. The two figures show that the presence of the test subject affects the dynamics of the system slightly.

The measured accelerance $h^s_{a,11}$ of the empty structure was curve fitted using the rational fraction polynomial method [35]. Good agreement between the curve-fitted (CF) accelereance and its measured counterpart is demonstrated in Fig. 11. The analytical expression of the curve-fitted accelerance is

$$h^s_{a,11}(s) = \frac{a_0 s^6 + a_1 s^5 + a_2 s^4 + a_3 s^3 + a_4 s^2 + a_5 s + a_6}{b_0 s^2 + b_1 s + b_2} \tag{28}$$

where $a_0 = 2.0486 \times 10^{-9}\ s^4$, $a_1 = -2.9053 \times 10^{-9}\ s^3$, $a_2 = 1.4985 \times 10^{-6}\ s^2$, $a_3 = -1.6243 \times 10^{-6} s$, $a_4 = -5.9928 \times 10^{-4}$, $a_5 = -2.1540 \times 10^{-4} s^{-1}$, $a_6 = 0.0266\ s^{-2}$, $b_0 = 1.8069\ N \cdot s^2 \cdot m^{-1}$, $b_1 = 0.1606\ N \cdot s \cdot m^{-1}$ and $b_2 = 412.8475\ N \cdot m^{-1}$.

The pair of eigenvalues corresponding to the first mode of the human-structure system were identified to be $-0.0536 \pm 14.9840i\ s^{-1}$ by curve fitting either the accelerance $h^{sh}_{a,11}$ or $h^{sh}_{a,21}$.

3.2.2. Dynamic properties of the human body

Based on the direct accelerance of the empty structure (Eq. (28)), the pair of eigenvalues of the occupied bridge and Eq. (27), the undamped frequency and damping ratio of the test subject were identified to be 4.85 Hz and 27.0%, respectively.

Fig. 6. A human and a shaker at TP1.

To validate the results, the accelerances $h^{sh}_{a,21}$ and $h^{sh}_{a,11}$ were synthesised using Eqs. (13) and (14). Figs. 12 and 13 show that the synthesised accelerances (thick dashed curves) of the human-structure system agree well with their measured counterparts (thin solid curves).

To further validate the results of the identification of human body dynamics, the nonlinear optimisation method [2] was employed. The natural frequency identified in this way was 4.84 Hz and damping ratio was 30.0%. These results are close to those identified by the proposed method, confirming its validity.

3.2.3. Discussion on the working of the method for identifying the dynamics of the human body

According to Eq. (27), theoretically, if the eigenvalues μ^{sh}_k and $\overline{\mu}^{sh}_k$ of the human-structure system are different from the eigenvalues μ^{s}_k and $\overline{\mu}^{s}_k$ of the empty structure, the damping and stiffness of the human can be identified. In practice, only a reliable detection of the eigenvalue difference between the unoccupied and occupied structures leads to reliable damping and stiffness. The eigenvalue difference is composed of the frequency and damping differences, which correspond to the changes of the peak frequency and magnitude of FRF, respectively. Hence, the working of the proposed method relies on the reliable detection of the changes of the peak frequency and magnitude of FRF.

A conservative criterion for reliable identification of two closely spaced spectral peaks states that the frequency separation between the two peaks should be at least twice the frequency resolution provided the rectangular window is used in signal processing [37]. The frequency separation is required to be four times greater than the frequency resolution in cases in which the Hann or Hamming window is used [37]. Therefore, the proposed method allows the reliable identification of human body dynamics if the frequency difference between the unoccupied and occupied structures is at least two times greater than the frequency resolution when the rectangular window is used in data processing or at least four times greater when the Hann or Hamming window is utilised.

Since the rectangular window was used in analysis of the human-structure system presented in Section 3.2 and the frequency separation of 0.03 Hz is approximately four times of the frequency resolution ($\Delta f = 1/128$ Hz), the identification of the human body dynamics is reliable in the example presented.

The structure (modal) to human mass ratio is one of the factors which affects the frequency difference [9]. Based on the criterion about the minimum frequency difference, the effect of the mass ratio may be investigated using parametric analysis. Let us consider the human-structure system presented in Section 3.2. Let us assume that the bridge has frequency of 2.41 Hz, damping ratio of 0.3% and varying modal mass while the properties of the human are as follows: mass 100 kg, frequency 4.85 Hz and damping ratio 27.0%. The frequency of the mode dominated by the structural motion of the joint system can be calculated (thick solid line in Fig. 14). The thick dashed line in Fig. 14 is separated by a distance of $2\Delta f$ (=0.0156 Hz) from the thick dash-dotted line, which indicates the frequency of the unoccupied system (2.41 Hz). The intersection of the thick solid line and the thick dashed line indicates that the frequency difference is greater than $2\Delta f$ for the mass ratio up to 98. For the human-structure system presented in Section 3.2, the mass ratio was 70, and therefore the human body dynamics were reliably identifiable.

The structure to human ratios for frequency and damping ratio are the other two factors affecting the frequency difference [9]. The parametric analysis for investigating the effect of the structure to human ratios for frequency and damping ratio is similar to that for the mass ratio and therefore it is not presented here.

4. Identification of the dynamics of the empty structure

In this section, formulas for the identification of the properties of the empty structure from the known dynamics of the human and human-structure system are presented. Their use is illustrated utilising the experiment described in Section 3.2 and a numerical example of a three-span glass FRP composite bridge.

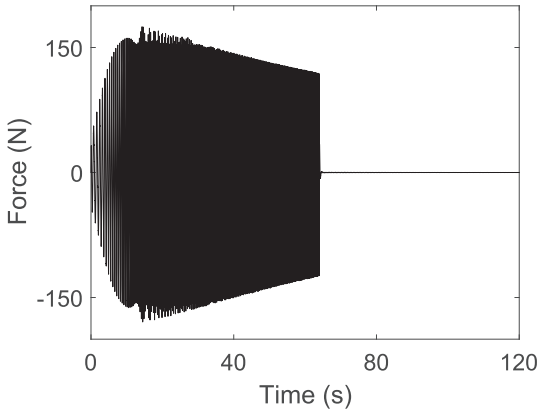

Fig. 7. Excitation force at TP1.

4.1. Theoretical derivations

Rearranging Eq. (14) generates the direct receptance of the unoccupied structure

$$h_{nn}^{s}(s)=\frac{\left(1+\frac{1}{m_h s^2}(c_h s+k_h)\right)h_{nn}^{sh}(s)}{1+\frac{1}{m_h s^2}(c_h s+k_h)-(c_h s+k_h)h_{nn}^{sh}(s)} \tag{29}$$

which is a function of the known direct receptance $h_{nn}^{sh}(s)$ of the human-structure system and the known dynamic properties of the human.

Rewriting (13) leads to

$$h_{pn}^{s}(s)=h_{pn}^{sh}(s)+\frac{h_{nn}^{s}(s)(c_h s+k_h)h_{pn}^{sh}(s)}{\left(1+\frac{1}{m_h s^2}(c_h s+k_h)\right)} \tag{30}$$

Substituting (29) into (30) results in

$$h_{pn}^{s}(s)=h_{pn}^{sh}(s)+\frac{h_{pn}^{sh}(s)(c_h s+k_h)h_{nn}^{sh}(s)}{1+\frac{1}{m_h s^2}(c_h s+k_h)-(c_h s+k_h)h_{nn}^{sh}(s)} \tag{31}$$

which shows that the cross receptance of the unoccupied structure could be deduced from the direct and cross receptance functions of the human-structure system and the dynamic properties of the human. The natural frequency and damping ratio of the unoccupied structure can then be calculated from the characteristic equation (i.e. denominator in Eq. (29) or (31) equated to zero).

As can be seen from Eqs. (29) and (31), the quality of the curve fitting of the FRFs around the modes dominated by structural motion of the joint system plays a key role in identifying the modes of the empty structure. The strategies for performing curve fitting have been investigated elsewhere, e.g. Refs. [35,36], and have not been elaborated in this paper.

4.2. The effect of uncertainties in the human body dynamics on the identification of the dynamic properties of the empty structure

The expectation and standard deviation of the magnitude of the $pn-$ th receptance of the empty structure system can be expressed as

$$E\left(\left|h_{pn}^{s}(s)\right|\right)\approx\left|h_{pn}^{s}(s)\right|\Big|_{\substack{c_h=E_{c_h}\\k_h=E_{k_h}}}+\frac{1}{2}\left(\frac{\partial^2\left|h_{pn}^{s}(s)\right|}{\partial c_h^2}\Big|_{\substack{c_h=E_{c_h}\\k_h=E_{k_h}}}\sigma_{c_h}^2+\frac{\partial^2\left|h_{pn}^{s}(s)\right|}{\partial k_h^2}\Big|_{\substack{c_h=E_{c_h}\\k_h=E_{k_h}}}\sigma_{k_h}^2\right) \tag{32}$$

and

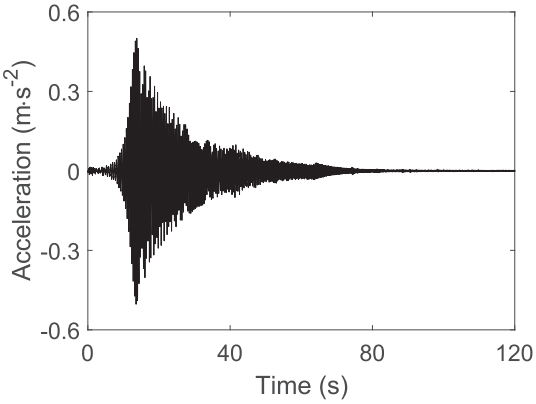

Fig. 8. Acceleration at TP1.

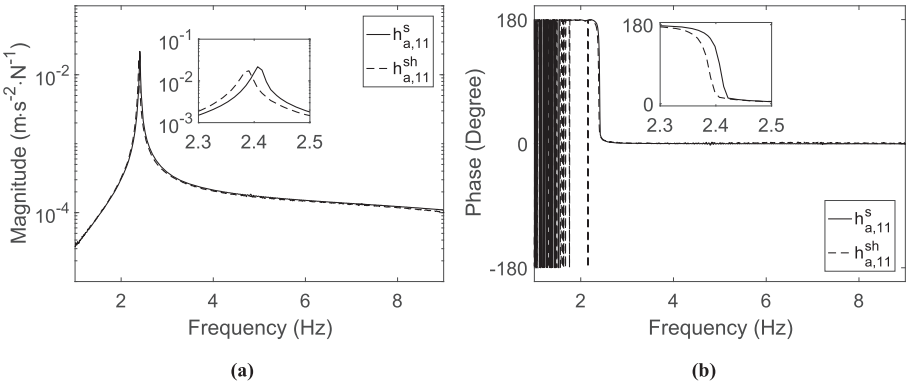

Fig. 9. Direct accelerances of the unoccupied and occupied structures: (a) Magnitude; (b) Phase.

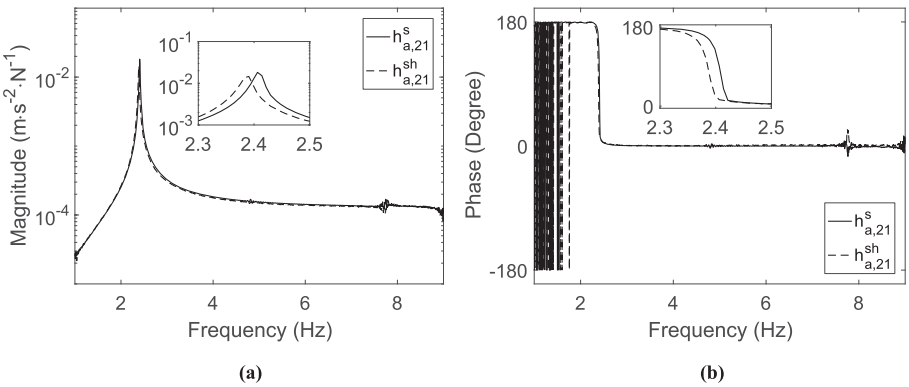

Fig. 10. Cross accelerances of the unoccupied and occupied structures: (a) Magnitude; (b) Phase.

$$\sigma\left(\left|h^s_{pn}(s)\right|\right) \approx \sqrt{\left(\frac{\partial\left|h^s_{pn}(s)\right|}{\partial c_h}\,\middle|\, \begin{matrix} c_h = E_{c_h} \\ k_h = E_{k_h} \end{matrix}\right)^2 \sigma^2_{c_h} + \left(\frac{\partial\left|h^s_{pn}(s)\right|}{\partial k_h}\,\middle|\, \begin{matrix} c_h = E_{c_h} \\ k_h = E_{k_h} \end{matrix}\right)^2 \sigma^2_{k_h}} \tag{33}$$

Similarly, the expectation and standard deviation of the phase of the $pn-$ th receptance of the empty structure system can be expressed as,

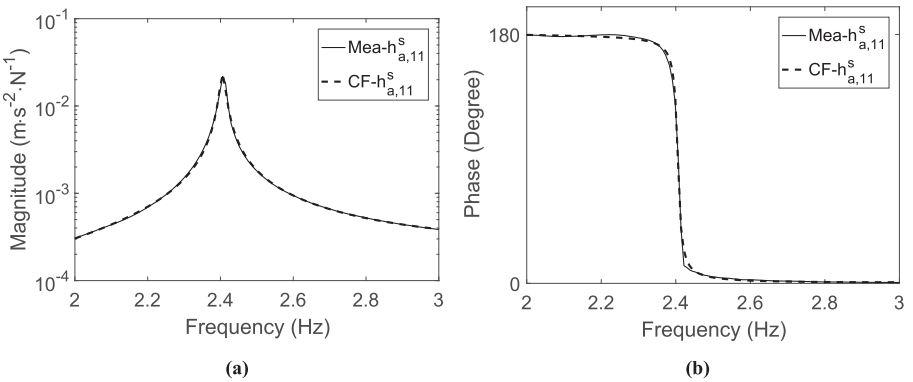

Fig. 11. Comparison between measured and curve-fitted accelerenace $h^s_{a,11}$: (a) Magnitude; (b) Phase.

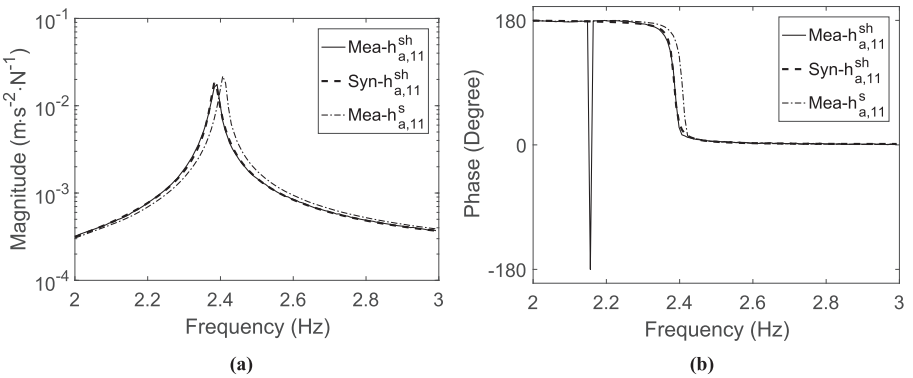

Fig. 12. Direct accelerances of unoccupied and occupied structures: (a) Magnitude; (b) Phase.

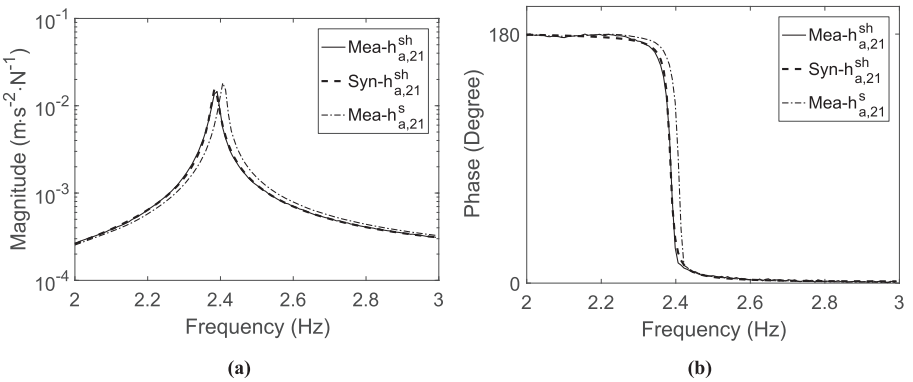

Fig. 13. Cross accelerances of unoccupied and occupied structures: (a) Magnitude; (b) Phase.

$$\mathrm{E}\left(\angle h^s_{pn}(s)\right) \approx \angle h^s_{pn}(s)\left|\begin{matrix} c_h = E_{c_h} \\ k_h = E_{k_h} \end{matrix}\right. + \frac{1}{2}\left(\frac{\partial^2 \angle h^s_{pn}(s)}{\partial c_h^2}\left|\begin{matrix} c_h = E_{c_h} \\ k_h = E_{k_h} \end{matrix}\right. \sigma^2_{c_h} + \frac{\partial^2 \angle h^s_{pn}(s)}{\partial k_h^2}\left|\begin{matrix} c_h = E_{c_h} \\ k_h = E_{k_h} \end{matrix}\right. \sigma^2_{k_h}\right) \tag{34}$$

and

$$\sigma\left(\angle h^s_{pn}(s)\right) \approx \sqrt{\left(\frac{\partial \angle h^s_{pn}(s)}{\partial c_h}\left|\begin{matrix} c_h = E_{c_h} \\ k_h = E_{k_h} \end{matrix}\right.\right)^2 \sigma^2_{c_h} + \left(\frac{\partial \angle h^s_{pn}(s)}{\partial k_h}\left|\begin{matrix} c_h = E_{c_h} \\ k_h = E_{k_h} \end{matrix}\right.\right)^2 \sigma^2_{k_h}} \tag{35}$$

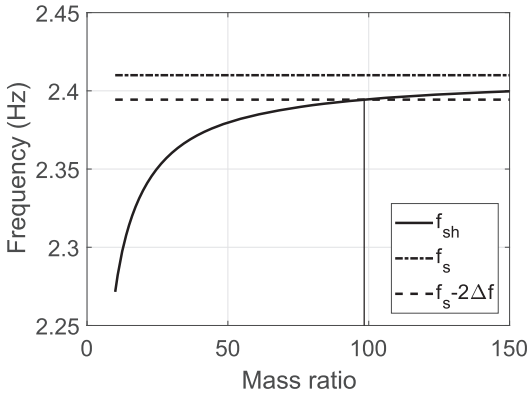

Fig. 14. Frequency of the mode dominated by structural motion against the modal mass of the structure to the human mass ratio ($\Delta f = 1/128$).

4.3. Experimental case study: dynamic properties of the structure

The use of the proposed method is demonstrated on an example of identifying the properties of the bridge from Section 3.2, by utilising the measured accelerances while the test subject was standing on the structure and known properties of the human. The measured direct and cross accelerances were curve fitted using the rational fraction polynomial method [35]. The analytical expression of the curve-fitted accelerance $h^{sh}_{a,11}(s)$ is

$$h^{sh}_{a,11}(s) = \frac{a_0 s^6 + a_1 s^5 + a_2 s^4 + a_3 s^3 + a_4 s^2 + a_5 s + a_6}{b_0 s^2 + b_1 s + b_2} \tag{36}$$

where $a_0 = 1.8385 \times 10^{-9}$ s^4, $a_1 = -1.7167 \times 10^{-9}$ s^3, $a_2 = 1.3257 \times 10^{-6}$ s^2, $a_3 = -9.7898 \times 10^{-7}$ s, $a_4 = 5.5414 \times 10^{-4}$, $a_5 = -1.4522 \times 10^{-4}$ s^{-1}, $a_6 = 0.0228$ s^{-2}, $b_0 = 1.8417$ N·s^2·m^{-1}, $b_1 = 0.1975$ N·s·m^{-1} and $b_3 = 413.5110$ N·m^{-1}.

The analytical expression of the curve-fitted accelerance $h^{sh}_{a,21}(s)$ is

$$h^{sh}_{a,21}(s) = \frac{a_0 s^6 + a_1 s^5 + a_2 s^4 + a_3 s^3 + a_4 s^2 + a_5 s + a_6}{b_0 s^2 + b_1 s + b_2} \tag{37}$$

where $a_0 = 1.8438 \times 10^{-9}$ s^4, $a_1 = -1.6904 \times 10^{-9}$ s^3, $a_2 = 1.3114 \times 10^{-6}$ s^2, $a_3 = -9.6580 \times 10^{-7}$ s, $a_4 = 5.4878 \times 10^{-4}$, $a_5 = -1.4277 \times 10^{-4}$ s^{-1}, $a_6 = 0.0225$ s^{-2}, $b_0 = 2.2058$ N·s^2·m^{-1}, $b_1 = 0.2366$ N·s·m^{-1} and $b_3 = 495.2469$ N·m^{-1}.

The accelerances $h^{s}_{a,11}$ and $h^{s}_{a,21}$ were then found using Eqs. (29) and (31). Figs. 15 and 16 show that the calculated accelerances (thick dashed lines) of the empty structure agree well with their measured counterparts (thin solid lines). Utilising the characteristic equation for the synthesised accelerances of the empty structure, the fundamental natural frequency and damping ratio of the empty structure were identified as 2.41 Hz and 0.3% (i.e. the same values that would be obtained by curve fitting the measured accelerance for the empty structure).

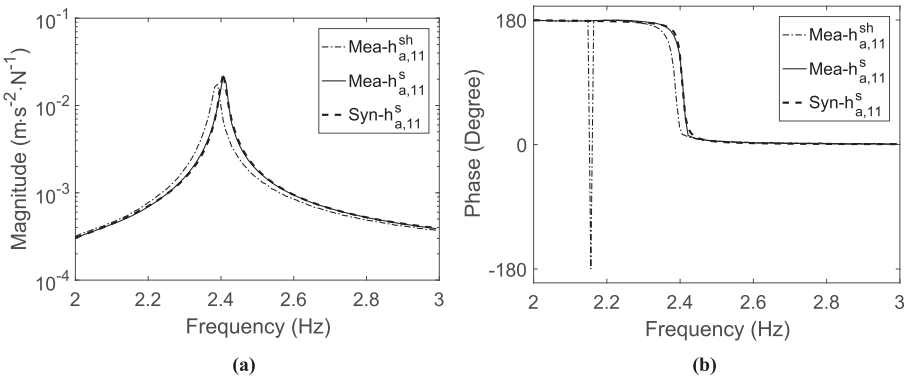

Fig. 15. Direct accelerances of unoccupied and occupied structures: (a) Magnitude; (b) Phase.

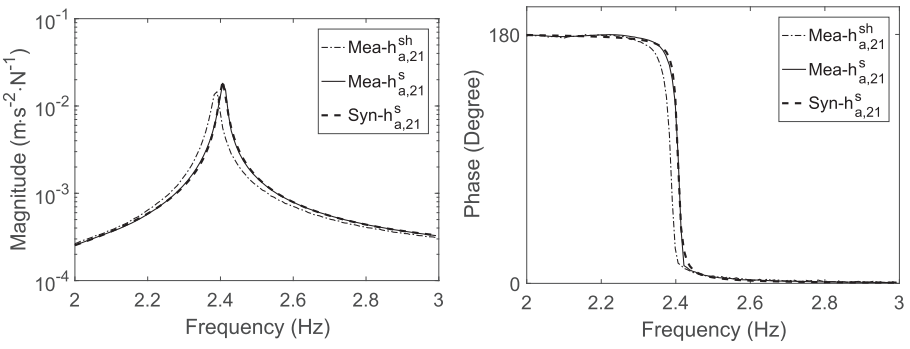

Fig. 16. Cross accelerances of unoccupied and occupied structures: (a) Magnitude; (b) Phase.

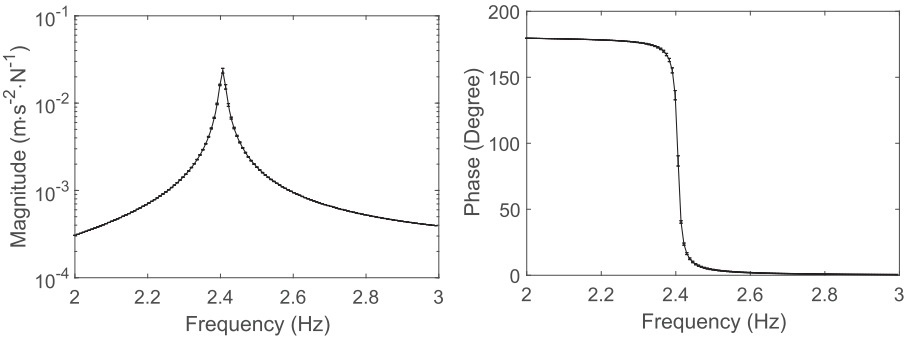

Fig. 17. Direct accelerance of the empty system: (a) Magnitude; (b) Phase; Solid line - Expectation; Error bar - Standard deviation.

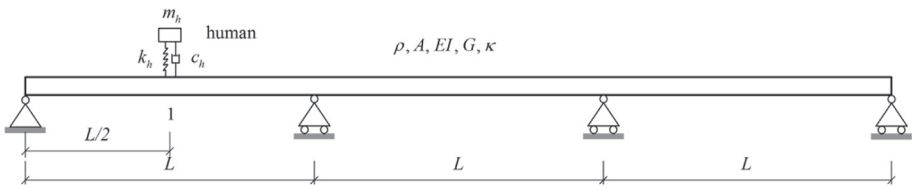

Fig. 18. A three-span continuous bridge.

Let the expectations of the damping and stiffness of the human body be $E_{c_h} = 1.65 \times 10^3\ \mathrm{N{\cdot}s{\cdot}m^{-1}}$ and $E_{k_h} = 9.28 \times 10^4\ \mathrm{N{\cdot}m^{-1}}$, respectively. Let us assume that the standard deviations of the damping and stiffness are $\sigma_{c_h} = 0.1c_h\ \mathrm{N{\cdot}s{\cdot}m^{-1}}$ and $\sigma_{k_h} = 0.1k_h\ \mathrm{N{\cdot}m^{-1}}$, respectively. The corresponding expectations and standard deviations of the damping ratio and frequency of the human body are $E_{\zeta_h} = 27.0\%$ and $\sigma_{\zeta_h} = 3.0\%$ and $E_{f_h} = 4.84$ Hz and $\sigma_{f_h} = 0.24$ Hz, estimated using the second-order perturbation method [32]. By using the proposed uncertainty estimation method, the expectation and standard deviation of the direct accelerance of the empty bridge are plotted in Fig. 17. The CoV of 10% for both the damping and stiffness of the human body led to the maximum CoV of 7% for the magnitude and phase of the predicted FRF of the empty structure. The predicted expectation and standard deviation of FRFs were verified using Monte Carlo simulations (sample size = 1000).

4.4. Numerical example: correcting multiple modes of a bridge

A three-span continuous bridge (Fig. 18) made of glass FRP composite material is used to illustrate the robustness of the method. The bridge has a total length of $3L = 3 \times 20 = 60$ m, density $\rho = 1.9 \times 10^3\ \mathrm{kg{\cdot}m^{-3}}$, area of cross section $A = 2.5 \times 10^{-2}\ \mathrm{m^2}$, longitudinal modulus of elasticity $E = 2.47 \times 10^{10}\ \mathrm{N{\cdot}m^{-2}}$, second moment of area $I = 2.0 \times 10^{-3}\ \mathrm{m^4}$,

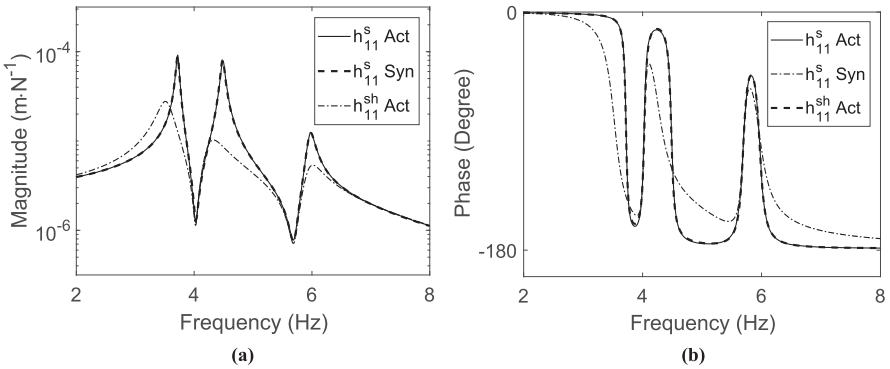

Fig. 19. Direct receptances of the occupied and unoccupied structures: (a) Magnitude; (b) Phase.

shear modulus $G = 3.9 \times 10^9$ N·m^{-2} and shear coefficient $\kappa = 0.08$. A human having mass $m_h = 73$ kg, natural frequency $f_h = 4.41$ Hz and damping ratio $\zeta_h = 33.0\%$ is assumed to stand in the middle of the first span (point 1 in Fig. 18).

A two-dimensional finite element (FE) model of the bridge is developed using an improved two-node Timoshenko beam finite element [38]. The FE model consists of 120 elements of equal length. Proportional damping $\mathbf{C} = \alpha\mathbf{M} + \beta\mathbf{K}$ ($\alpha = \beta = 0.0006$) is assumed. Similarly, the FE model of the human-bridge system can be obtained.

Numerical integration was first carried out to calculate the time-domain responses of the human-bridge system driven by a linear chirp excitation force (having magnitude 100 N and sweeping from 1 Hz to 10 Hz) at point 1 for 112 s and then left to return to rest over the next 8 s. The actual direct receptance h_{11}^{sh} of the human-bridge system was then numerically estimated using the excitation force and the resultant vertical displacement response at point 1 and it is shown by the thin dash-dotted line in Fig. 19. This receptance plays the role of a known (usually by measurement) FRF of the human-structure system. By curve fitting the receptance h_{11}^{sh} in the frequency range from 2 Hz to 8 Hz, a rational fraction polynomial of the direct receptance may be obtained as

$$h_{11}^{sh}(s) = \frac{\sum_{i=1}^{13} a_{i-1} s^{13-i}}{\sum_{j=1}^{9} b_{j-1} s^{9-j}} \tag{38}$$

where $a_{i-1} (i = 1, 2, \ldots, 13)$ and $b_{j-1} (j = 1, 2, \ldots, 9)$ are given the appendix. Its characteristic equation gives the natural frequencies and damping ratios of the first four modes of the human-bridge system, which are summarised in Table 2.

By using the proposed method, the known human body dynamics, Eqs. (38) and (29), the direct receptance of the unoccupied bridge in the frequency range from 2 Hz to 8 Hz can be synthesised, shown by the thick dashed line in Fig. 19. It can be seen that the synthesised receptance of the unoccupied bridge is coincident with the actual receptance (denoted as Act in Fig. 19) of the unoccupied bridge (the thin solid line in Fig. 19), which was obtained numerically. The natural frequencies and damping ratios of the unoccupied bridge were then determined by solving the characteristic equation obtained from the synthesised direct receptance of the unoccupied bridge and they are presented in Table 2.

The occupancy of the human increases the damping ratios of the first three structural motion dominated modes by 443%, 413% and 145%, respectively (Table 2). By contrast, it decreases the frequencies of the first three modes by 5.1%, 5.1% and 0.3%, respectively. This example demonstrates that had the measured human-structure receptances not been corrected, the modal properties of the structure would be erroneous.

Table 2
Modal parameters of the human-bridge system and the unoccupied bridge (S Mode - Structural motion dominated mode; H Mode - Human motion dominated mode).

No.	Mode Description	Human-bridge system		Empty bridge		Relative difference (%)	
		Frequency (Hz)	Damping ratio (%)	Frequency (Hz)	Damping ratio (%)	Frequency	Damping ratio
1	S Mode	3.53	3.8	3.72	0.7	−5.1	443
2	S Mode	4.25	4.1	4.48	0.8	−5.1	413
3	H Mode	5.00	23.8	/	/	/	/
4	S Mode	5.95	2.7	5.97	1.1	−0.3	145

Fig. 19 shows that the proposed method corrects the dynamic properties of the first three modes (two of which are relatively closely spaced) simultaneously which is advantageous compared with the methods that rely on SDOF models of the structure.

5. Conclusions

The paper presents a new theoretical framework which offers closed-form solutions in terms of curve-fitted FRFs and flexibility of being used for any of the three applications as and when needed, i.e. prediction of the dynamics of a structure occupied by a human when the properties of individual components are known, the identification of human body dynamics when the dynamics of the empty structure and the structure occupied by the human are known and the identification of the empty structure when the dynamics of the human and the structure occupied by the human are known. In addition, the influence of uncertainties in human body dynamics on the dynamic identification of the empty structure and human-structure system was quantified using the second-order perturbation method. The robustness and accuracy of the proposed framework were demonstrated in several numerical and experimental examples. The method is simple to use, it is computationally efficient and it provides an effective means of studying human-structure interaction problems that are especially relevant for light-weight, slender structures. The proposed method, which focuses on the presence of a single human in this paper, will be extended to the crowd-structure interaction in future work.

Acknowledgment

This research work was supported by the UK Engineering and Physical Sciences Research Council [grant number EP/M021505/1: Characterising dynamic performance of fibre reinforced polymer structures for resilience and sustainability]. The data are self-contained in the paper.

Appendix. Coefficients in Eq. (38)

$a_0 = -2.1394\times10^{-23}\,\mathrm{s}^{10}$, $a_1 = 5.0748\times10^{-21}\,\mathrm{s}^{9}$, $a_2 = -9.3199\times10^{-19}\,\mathrm{s}^{8}$, $a_3 = 3.8819\times10^{-17}\,\mathrm{s}^{7}$, $a_4 = 2.5281\times10^{-15}\,\mathrm{s}^{6}$, $a_5 = 2.6507\times10^{-13}\,\mathrm{s}^{5}$, $a_6 = 1.1073\times10^{-10}\,\mathrm{s}^{4}$, $a_7 = 2.2661\times10^{-9}\,\mathrm{s}^{3}$, $a_8 = 2.8389\times10^{-07}\,\mathrm{s}^{2}$, $a_9 = 3.6935\times10^{-6}\,\mathrm{s}$, $a_{10} = 2.4034\times10^{-4}$, $a_{11} = 0.0015\,\mathrm{s}^{-1}$, $a_{12} = 0.0658\,\mathrm{s}^{-2}$, $b_0 = 4.4691\times10^{-8}\,\mathrm{N\cdot s^{8}\cdot m^{-1}}$, $b_1 = 9.2806\times10^{-7}\,\mathrm{N\cdot s^{7}\cdot m^{-1}}$, $b_2 = 1.6473\times10^{-4}\,\mathrm{N\cdot s^{6}\cdot m^{-1}}$, $b_3 = 0.0024\,\mathrm{N\cdot s^{5}\cdot m^{-1}}$, $b_4 = 0.2132\,\mathrm{N\cdot s^{4}\cdot m^{-1}}$, $b_5 = 1.9781\,\mathrm{N\cdot s^{3}\cdot m^{-1}}$, $b_6 = 114.5197\,\mathrm{N\cdot s^{2}\cdot m^{-1}}$, $b_7 = 496.7671\,\mathrm{N\cdot s\cdot m^{-1}}$ and $b_8 = 2.1588\times10^{4}\,\mathrm{N\cdot m^{-1}}$.

References

[1] B.R. Ellis, T. Ji, Human-structure interaction in vertical vibrations, Proc. Inst. Civ. Eng. Struct. Build. 122 (1997) 1–9.
[2] R. Sachse, The Influences of Human Occupants on the Dynamic Properties of Slender Structures, PhD Thesis, University of Sheffield, 2003.
[3] R. Sachse, A. Pavic, P. Reynolds, Human-structure dynamic interaction in civil engineering dynamics: a literature review, Shock Vib. Digest 35 (2003) 3–18.
[4] E. Shahabpoor, A. Pavic, V. Racic, Interaction between walking humans and structures in vertical direction: a lterature review, Shock Vib. 2016 (2016) 22.
[5] K. Van Nimmen, G. Lombaert, G. De Roeck, P. Van den Broeck, Reduced-order models for vertical human-structure interaction, J. Phys. Conf. Ser. 744 (2016) 012030.
[6] X. Zheng, J.M.W. Brownjohn, Modeling and simulation of human-floor system under vertical vibration, in: L.P. Davis (Ed.), Proc. SPIE 4327, Smart Structures and Materials 2001: Smart Structures and Integrated Systems, Newport Beach, CA, USA, 2001, pp. 513–520.
[7] K. Van Nimmen, G. Lombaert, G. De Roeck, P. Van den Broeck, The impact of vertical human-structure interaction on the response of footbridges to pedestrian excitation, J. Sound Vib. 402 (2017) 104–121.
[8] P. Reynolds, A. Pavic, Z. Ibrahim, Changes of modal properties of a stadium structure occupied by a crowd, in: Proceedings of the 22nd International Modal Analysis Conference, 2004, pp. 421–428.
[9] R. Sachse, A. Pavic, P. Reynolds, Parametric study of modal properties of damped two-degree-of-freedom crowd–structure dynamic systems, J. Sound Vib. 274 (2004) 461–480.
[10] J. Sim, A. Blakeborough, M. Williams, Modelling effects of passive crowds on grandstand vibration, Proc. Inst. Civ. Eng. Struct. Build. 159 (2006) 261–272.
[11] J.M.W. Brownjohn, Energy dissipation from vibrating floor slabs due to human-structure interaction, Shock Vib. 8 (2001).
[12] S.H. Kim, K. Cho, M. Choi, M.S. Choi, J.Y. Lim, Development of human body model for the dynamic analysis of footbridges under pedestrian induced excitation, Steel Struct. 8 (2008) 333–345.
[13] E. Shahabpoor, A. Pavic, V. Racic, Identification of mass–spring–damper model of walking humans, Structures 5 (2016) 233–246.
[14] K. Van Nimmen, K. Maes, S. Zivanovic, G. Lombaert, G. De Roeck, P. Van den Broeck, Identification and modelling of vertical human-structure interaction, in: J. Caicedo, S. Pakzad (Eds.), Dynamics of Civil Structures, Volume 2: Proceedings of the 33rd IMAC, a Conference and Exposition on Structural Dynamics, 2015, Springer International Publishing, Cham, 2015, pp. 319–330.
[15] C.C. Caprani, E. Ahmadi, Formulation of human–structure interaction system models for vertical vibration, J. Sound Vib. 377 (2016) 346–367.
[16] M. Zhang, C.T. Georgakis, W. Qu, J. Chen, SMD model parameters of pedestrians for vertical human-structure interaction, in: J. Caicedo, S. Pakzad (Eds.), Dynamics of Civil Structures, Volume 2: Proceedings of the 33rd IMAC, a Conference and Exposition on Structural Dynamics, 2015, Springer International Publishing, Cham, 2015, pp. 311–317.
[17] L. Wei, M.J. Griffin, Mathematical models for the apparent mass of the seated human body exposed to vertical vibration, J. Sound Vib. 212 (1998) 855–874.
[18] Y. Matsumoto, M.J. Griffin, Mathematical models for the apparent masses of standing subjects exposed to vertical whole-body vibration, J. Sound Vib. 260 (2003) 431–451.
[19] R.O. Foschi, G.A. Neumann, F. Yao, B. Folz, Floor vibration due to occupants and reliability-based design guidelines, Can. J. Civ. Eng. 22 (1995) 471–479.

[20] C.A. Jones, P. Reynolds, A. Pavic, Vibration serviceability of stadia structures subjected to dynamic crowd loads: a literature review, J. Sound Vib. 330 (2011) 1531–1566.
[21] Y. Matsumoto, M.J. Griffin, Dynamic response of the standing human body exposed to vertical vibration: influence of posture and vibration magnitude, J. Sound Vib. 212 (1998) 85–107.
[22] J. Sim, Human-structure Interaction in Cantilever Grandstands, PhD Thesis, The University of Oxford, 2006.
[23] A. Kyprianou, J.E. Mottershead, H. Ouyang, Assignment of natural frequencies by an added mass and one or more springs, Mech. Syst. Signal Process. 18 (2004) 263–289.
[24] X. Wei, J.E. Mottershead, Y.M. Ram, Partial pole placement by feedback control with inaccessible degrees of freedom, Mech. Syst. Signal Process. 70–71 (2016) 334–344.
[25] X. Wei, J.E. Mottershead, Block-decoupling vibration control using eigenstructure assignment, Mech. Syst. Signal Process. 74 (2016) 11–28.
[26] X. Wei, J.E. Mottershead, Aeroelastic systems with softening nonlinearity, AIAA J. 52 (2014) 1915–1927.
[27] IStructE/DTLR/DCMS, Dynamic Performance Requirements for Permanent Grandstands Subject to Crowd Action, Recommendations for Management, Design and Assessment, The Institution of Structural Engineers (IStructE), London, 2008.
[28] A. Pavic, P. Reynolds, Experimental verification of novel 3DOF model for grandstand crowdstructure dynamic interaction, in: 26th International Modal Analysis Conference: IMAC-XXVI, Orlando, Florida, 2008.
[29] C.A. Jones, A. Pavic, P. Reynolds, R.E. Harrison, Verification of equivalent mass–spring–damper models for crowd–structure vibration response prediction, Can. J. Civ. Eng. 38 (2011) 1122–1135.
[30] K.A. Salyards, N.C. Noss, Experimental evaluation of the influence of human-structure interaction for vibration serviceability, J. Perform. Constr. Facil. 28 (2014) 458–465.
[31] G.H. Golub, C.F. Van Loan, Matrix Computations, third ed., Johns Hopkins, Baltimore, MD, 1996.
[32] B. Sudret, Uncertainty propagation and sensitivity analysis in mechanical models–Contributions to structural reliability and stochastic spectral methods, Habilitationa diriger des recherches, Université Blaise Pascal, Clermont-Ferrand, France, 2007.
[33] ISO, ISO 5982:1981 Vibration and Shock – Mechanical Driving Point Impedance of the Human Body, International Organisation for Standarisation (ISO), Geneva, Switzerland, 1981.
[34] S. Zivanovic, X. Wei, J. Russell, J.T. Mottram, Vibration performance of two FRP footbridge structures in the United Kingdom, in: Footbridge 2017, Berlin, Germany, 2017.
[35] M.H. Richardson, D.L. Formenti, Parameter estimation from frequency response measurements using rational fraction polynomials, in: The 1st Internation Modal Analysis Conference, Orlando, FL, 1982.
[36] D. Formenti, M.H. Richardson, Global frequency & damping estimates from frequency response measurements, in: 4th International Modal Analysis Conference, Los Angeles, CA, 1986.
[37] M. Abe, J.O. Smith III, Design criteria for simple sinusoidal parameter estimation based on quadratic interpolation of FFT magnitude peaks, in: Audio Engineering Society Convention 117, Audio Engineering Society, 2004.
[38] Z. Friedman, J.B. Kosmatka, An improved two-node Timoshenko beam finite element, Comput. Struct. 47 (1993) 473–481.